Construction and Building Materials 57 (2014) 163–168

Contents lists available at ScienceDirect

Construction and Building Materials

journal homepage: www.elsevier.com/locate/conbuildmat

A feasibility study of strain hardening fiber reinforced fly ash-based geopolymer composites

Motohiro Ohno, Victor C. Li *

Department of Civil and Environmental Engineering, University of Michigan, Ann Arbor, MI 48109-2125, United States

HIGHLIGHTS

- Strain-hardening ductile fly ash-based geopolymer composite was demonstrated.
- The tensile ductility of the composite could reach over 4%.
- Crack pattern analysis was conducted by Digital Image Correlation.
- The maximum and average crack widths are 117 and 45 μm, respectively, at 4.5% strain.

ARTICLE INFO

Article history:
Received 20 January 2014
Accepted 4 February 2014

Keywords:
Geopolymer
Fly ash
Strain hardening
Fiber reinforced composite
Digital Image Correlation

ABSTRACT

Fly ash-based geopolymer has been intensively studied as a promising alternative to ordinary cement materials. While geopolymer concrete has good strength and excellent material greenness, applications have been limited to niche or small scale applications. In order to use geopolymer for large scale structural applications, the inherent brittleness should be addressed. In this study, strain-hardening ductile fiber reinforced geopolymer composites were developed by using randomly oriented short Poly-Vinyl Alcohol (PVA) fibers. Subsequently, their mechanical properties were investigated by cube compressive and dogbone tensile testing. Tensile strain hardening behavior with very high ductility of over 4% was experimentally demonstrated for the developed composites. These performances were found to be further improved by utilizing temperature curing methods. Crack width distributions were also investigated by using the Digital Image Correlation technique. The analysis indicated that the maximum and average crack widths are 117 μm and 45 μm, respectively, even at a high imposed strain level of 4.5%. Therefore, the feasibility of strain-hardening ductile geopolymer composites was established.

1. Introduction

The greenness potential of geopolymer, a promising alternative binder material to Ordinary Portland Cement (OPC), has so far not been fully realized in practice. Compared to cement manufacturing, which contributes 5–8% of the global emission of man-made CO_2, geopolymer production has 80% less carbon and 30% less energy footprints [1–3]. Moreover, industrial byproducts such as fly ash and slag can be utilized as source materials that are activated by alkaline solution to form geopolymer. Despite the outstanding environmental friendliness of geopolymer, however, use of geopolymer has to date been limited to niche applications or small scale products. To make the most of the excellent material greenness of geopolymer, large-scale applications in the construction industry should be seriously considered.

Over the last few decades, significant efforts have been made in the research community for understanding reaction mechanisms, chemistry and engineering properties of geopolymers. It has been found that fly ash-based geopolymer can exhibit better compressive strength and higher chemical, fire/temperature and frost resistance than OPC materials [4]. Geopolymer, however, is inherently brittle like conventional cement materials. Considering the large-scale applications, it is highly possible that the structural size effect resulting from material brittleness becomes significant. Further, as in OPC, a lack of structural durability will likely result if cracking in geopolymer is pervasive. Thus, a major step towards large-scale structural applications of geopolymer is to suppress its brittleness.

Fiber reinforcing has demonstrated to be highly effective in controlling the brittleness of cementitious materials. While fiber reinforced concrete (FRC) has enhanced fracture toughness, the

* Corresponding author. Tel.: +1 734 764 3368.
E-mail address: vcli@umich.edu (V.C. Li).

http://dx.doi.org/10.1016/j.conbuildmat.2014.02.005
0950-0618/

Table 1
Mix proportion of fiber reinforced fly ash-based geopolymer.

Fly ash A	Fly ash B	Sand	Na_2SiO_3	NaOH (pellet)	Pre-mix water	Mix water	Fiber (vol.%)
0.8	0.2	0.3	0.256	0.056	0.039	0.12	2

Table 2
Chemical compositions and physical properties of fly ash.

	Fly ash A	Fly ash B
SiO_2	46.06–47.07	43.39–44.09
Al_2O_3	22.55–23.42	23.21–24.24
Fe_2O_3	17.69–19.03	7.98–8.39
CaO	3.55–3.91	13.22–14.04
SO_3	0.25–0.52	1.31–1.46
Loss on ignition	2.10–3.75	0.56–1.26
Fineness (% retained on 45 μm sieve)	13.80–15.00	16.85–19.13

material remains quasi-brittle. Over the last decades, the development of strain hardening cementitious composites (SHCC) has gained significant attention worldwide [5–7]. As example, Engineered Cementitious Composites (ECC), a micromechanics-based designed ultra-ductile SHCC, has demonstrated tensile strain capacity about 300% higher than plain concrete. Further, the self-controlled tight crack width contributes to improvement in durability due to lower permeability of water and chloride ions and better self-healing property even when damaged, as a result of crack width limited to below 60 μm. In addition, the deliberate choice of short fibers with moderate fiber volume fraction (less than 2%) in ECC is advantageous in field applications. These excellent properties have led to a number of full-scale applications of ECC in the building and transportation industries to date.

Previous research on fiber reinforcing geopolymer showed improvement in fracture toughness, tensile ductility and strength [8–13]. However, large fiber volume fractions or complicated processing methods such as extrusion are often employed, thus limiting the economics and field applicability of such geopolymer-based composites. While some studies demonstrated enhanced ductility using short fibers with moderate volume fractions, further improvement would be possible by utilizing the micromechanics-based design method originally developed for ECC. Lee et al. applied the micro-mechanical modeling concept to fiber reinforced alkali-activated slag mortar, and experimentally demonstrated the very high tensile ductility and tightly controlled crack width [14]. It is therefore hypothesized that the micromechanics-based design methodology holds promise to achieving ultra-ductile fiber reinforced geopolymer composites that can be placed in field conditions and provide improved structural durability.

The present paper reports a feasibility study of strain hardening fiber reinforced fly ash-based geopolymer composites with very high tensile ductility and tight crack width. Appropriate mix proportions are determined through experiments, utilizing knowledge obtained from ECC development. Mechanical tests are then conducted to characterize the compressive and tensile strength, tensile behavior, and tensile strain capacity. In addition, the tensile crack pattern is investigated by Digital Image Correlation (DIC) technique, providing information on the number of cracks and crack width distribution over a given gage length at any strain level under load.

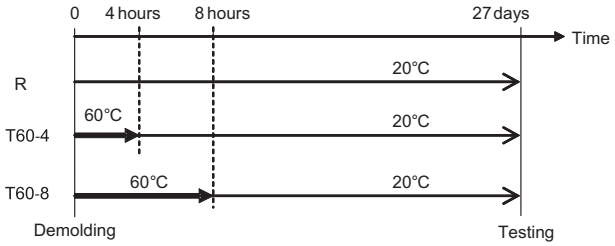

Fig. 1. Demolding 24 h after casting.

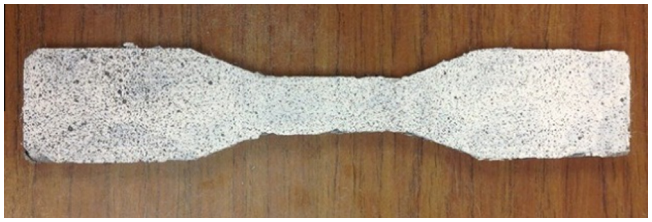

Fig. 2. Random speckle patterns make unique gray scale distributions in each specimen subset.

2. Experimental investigation

2.1. Materials and mix proportions

The mix proportion of geopolymer mortar was first determined through trial mixing so that the mortar has good mechanical properties, moderate setting time and adequate rheology for fiber dispersion. Poly-Vinyl Alcohol (PVA) fibers were employed with a volume fraction of 2%. Table 1 lists the resultant mix proportion of the geopolymer composite. The ratio is in terms of weight of the ingredients, except for the fiber that is expressed in terms of volume fraction. Two types of fly ash were used in this study, labeled Fly ash A and B, respectively. Fly ash A was obtained from Headwaters Resources and Fly ash B from Lafarge. Both are classified as class F fly ash as designated by ASTM C 618. Table 2 lists the chemical compositions and physical properties of fly ashes reported from each manufacturer. Slight variation is found in the reported data depending on the report date.

The purpose of using two types of fly ash is to control the hardening property of geopolymer mortar. When the fly ash A is singly used as the reactant, the specimens did not stiffen enough and fractured in demolding one day after casting. On the other hand, the use of fly ash B by itself resulted in too fast setting time to cast in molds. These problems might be related to the different amount of CaO content between Fly ash A and B, but further investigation would be required.

The alkaline activator consists of sodium silicate solution with 8.9 wt% Na_2O, 28.7 wt% SiO_2, and 62.5 wt% H_2O, laboratory-grade sodium hydroxide in pellet forms, and pre-mix tap water. Sodium silicate solution and pre-mix water were first mixed, and sodium hydroxide pellets were then dissolved in the solution. The solution preparation was done 24 h before its use as activator for geopolymer, as recommended in the research community, so that chemical equilibrium is attained. Additional water (labeled "Mix water" in Table 1) was used when mixed with solid materials (fly ash, silica sand and fiber) to obtain adequate rheology. As in most ECC materials, fine silica sand with an average diameter of 110 μm was used as aggregate and PVA fibers with 1.2% oil coating by weight were employed. Fiber properties are listed in Table 3.

Table 3
Properties of PVA fiber.

Fiber type	Nominal strength (MPa)	Apparent strength[a] (MPa)	Diameter (μm)	Length (mm)	Young's modulus (GPa)	Elongation (%)
REC 15	1620	1092	39	12	42.8	6.0

[a] Strength of fibers embedded in a cement matrix is lower than that in standard fiber strength testing.

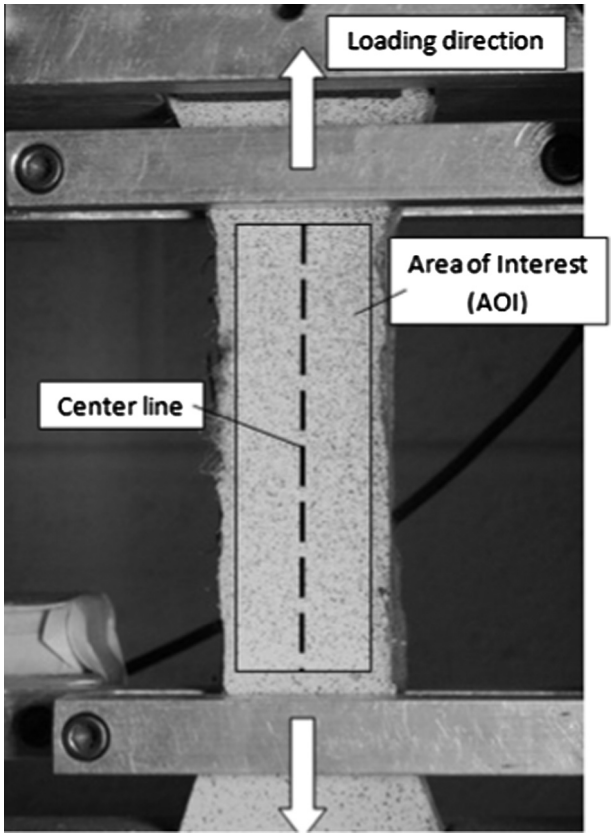

Fig. 3. Crack widths are computed from the strain values along the centerline.

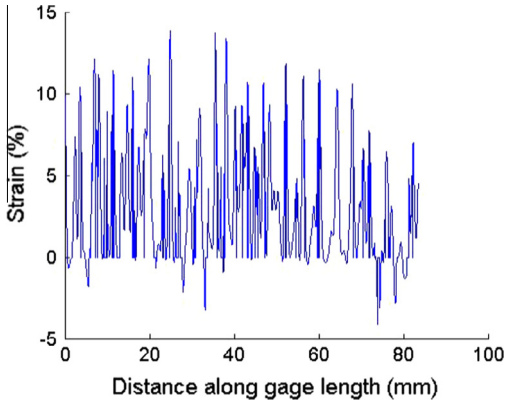

Fig. 4. Positive peaks in the strain distribution along the centerline correspond to cracks.

Table 4
Mechanical properties of R, T60-4 and T60-8 at the age of 28 days.

Specimens group ID	Compressive strength (MPa)	Tensile strength (MPa)	Tensile strain capacity (%)
R	17.4 ± 0.7	2.9 ± 0.3	2.7 ± 0.2
T60-4	20.9 ± 1.1	3.2 ± 0.3	3.8 ± 0.5
T60-8	27.6 ± 1.7	3.4 ± 0.5	4.3 ± 0.3

2.2. Mixing and curing

Fly ash A and B and micro-silica sand were first mixed in a 3 L Hobart mixer. The activator solution was then added, followed by the addition of mix water. After the mortar mixture reached the desired fresh state, PVA fibers were slowly added and then mixed until fibers were properly distributed. The mixture was cast into molds on a vibration table, and all specimens were demolded after 24 h.

Specimens were then divided into three groups and cured in three different conditions in order to investigate effects of curing temperature. Fig. 1 illustrates the curing methods used for each specimens group. The first group, labeled "R", was air cured at a room temperature (23 ± 3 °C) until the age of 28 days when mechanical tests were conducted. The second and third groups ("T60-4" and "T60-8") were first cured in an oven at 60 °C for 4 and 8 h, respectively. They were then air cured at a room temperature until the age of 28 days prior to testing.

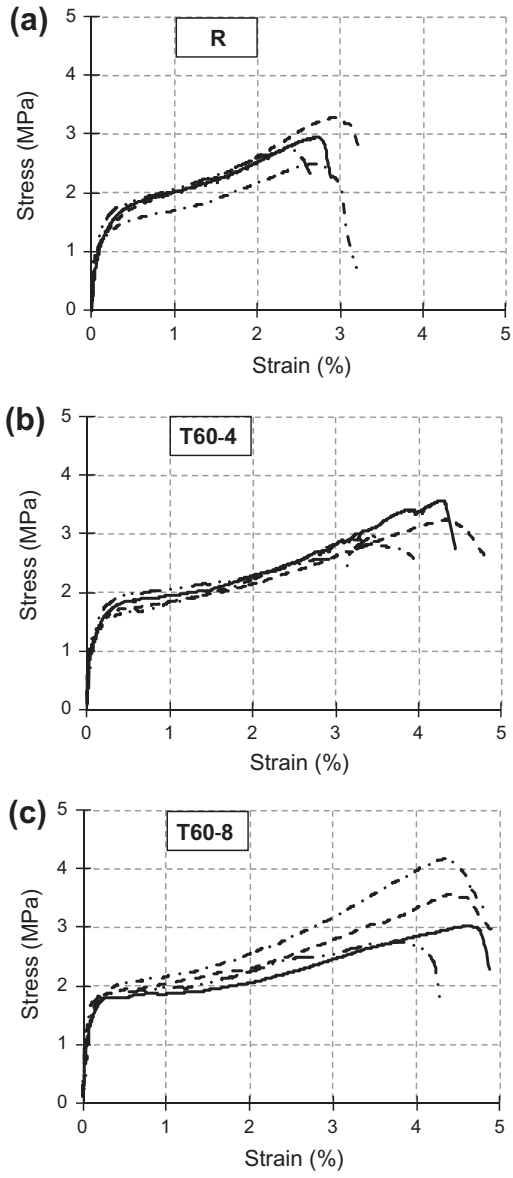

Fig. 5. Strain hardening behavior with high ductility is clearly seen in all cases.

2.3. Mechanical testing

Mechanical properties of prepared specimens were tested 28 days after casting. For each group experiencing different curing conditions, three 2 inch (50 mm) cube specimens and four dogbone-shaped specimens were prepared and subjected to uniaxial compression and tension testing, respectively. Dogbone testing was conducted following the test method recommended by Japan Society of Civil Engineers (JSCE) [15]. Specimens were subjected to quasi-static uniaxial tension loading under displacement control at the rate of 0.5 mm/min. Two LVDTs attached on each specimen measured extensions within the gage length of about 100 mm. Tensile strain was computed from the average of extensions divided by the gage length. The actual specimen geometry used in this study can be found in the literature [16].

2.4. Crack pattern analysis

Crack pattern analysis was conducted by using Digital Image Correlation (DIC) technique. DIC is a non-contact measurement method to analyze surface displacement/strain within an area of interest (AOI) of an object. Digital images of undeformed and deformed states are captured and compared in terms of the grey level of each pixel. In digital images, each pixel contains its grey scale data ranging from 0 to 255. Small regions (called subsets) consisting of a set of pixels are tracked before and after deformation by matching their grey scale distribution. The displacement/strain field is then computed from the movement of subsets. Various correlations functions can be used in the matching process, and interpolation functions are generally used for higher accuracy. The detailed theory can be found in the literature [17]. The biggest advantage of DIC technique is that it can provide full-field surface displacement/strain fields with high resolution, which has been quite difficult to be accomplished by conventional measurement equipment such as strain gages. DIC has been successfully applied to date in strain distribution analysis or crack propagation observations of cement materials [18–20].

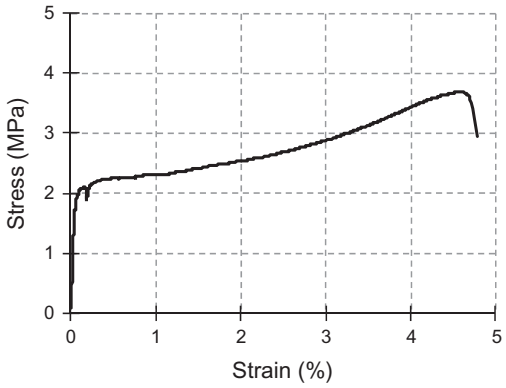

Fig. 6. Stress–strain curve of a specimen analyzed by DIC.

For the DIC analysis, additional dogbone specimens were prepared and cured in the same condition as the T60-8 group. Random speckle patterns were then created on the specimen surface by white and black spray painting so that each subset has a unique grey scale distribution [Fig. 2]. During tensile testing, a digital camera was mounted on a tripod in front of the testing machine, and digital images were taken at a five-second interval by using a remote control. In this study, 2-D image correlation analysis was conducted to measure in-plane deformations by using a commercial software Vic2D. Out-of-plane displacements were assumed to be sufficiently small because of the uniaxial tension testing configuration and the relatively small thickness of specimens compared to other dimensions.

Two major purposes of DIC analysis in the present study are (1) to obtain visual images of multiple cracking pattern development, and (2) to compute crack width distributions. Fig. 3 illustrates the testing configuration. Strain values within the AOI are calculated through the DIC analysis. Strain maps of loaded specimens can be obtained for digital images taken at a certain time interval. Since cracked regions have much larger strain values than uncracked ones, cracks can be easily visualized by a map of strain contours. In addition, crack width can be computed from the strain map. When multiple cracks are generated, strain distributions along the loading direction have peaks as shown in Fig. 4. Since the elastic strain of uncracked regions is more than one order of magnitude smaller than strain of cracked regions, the positive peak strain value is mainly attributed to the crack width at the

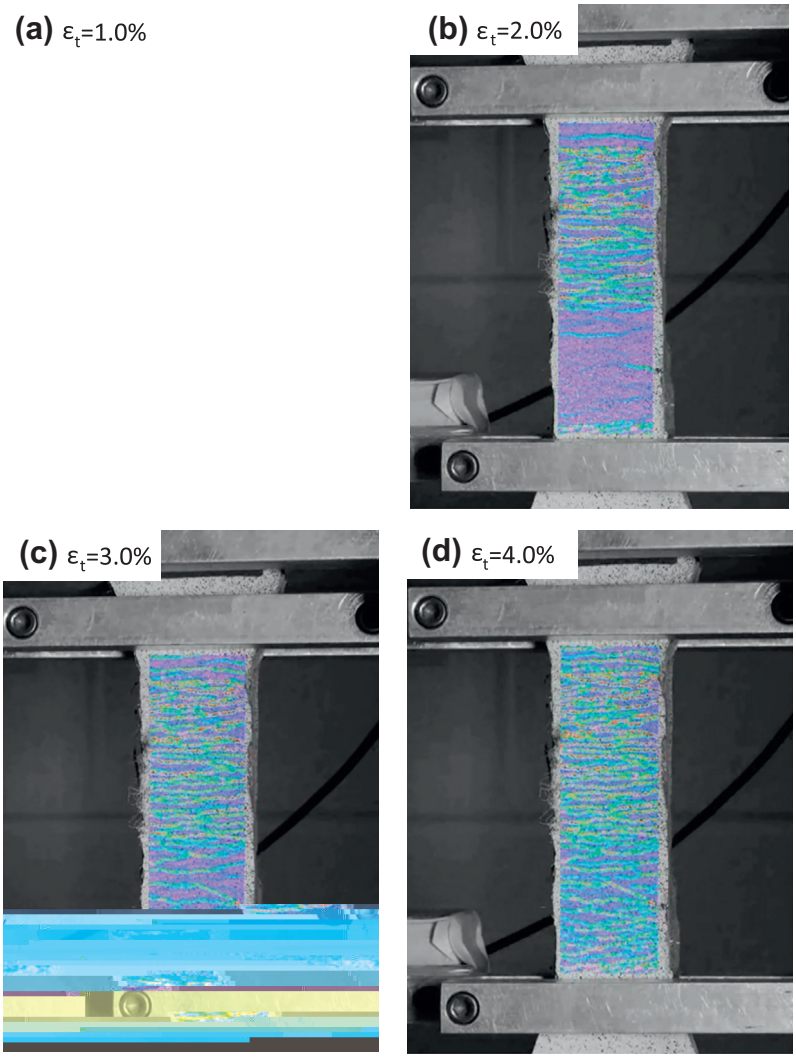

Fig. 7. Strain maps illustrate multiple crack formation at progressively increased imposed strain.

corresponding location. Several negative peaks are also seen; these are caused by computational errors or from special subsets adjacent to a crack experiencing relative contraction. It should be noted that the resolution of images was around 30 μm per pixel and the step of sampling points for strain calculation is 2, i.e. 60 μm interval. Since ordinary crack spacing in ECC materials is in the order of mm, each peak should correspond to a single crack. Therefore, each crack width can be calculated by integrating strain with respect to length over the peak. However, even in uncracked regions, some fluctuation in the strain distribution because of the heterogeneity of the material can be expected. Therefore, small peaks should not be counted as a crack if their computed crack width is too small. In this study, cracks with larger than 20 μm width are considered. Also, since peaks might include such inherent fluctuations, the computed crack width can be larger than the actual value. However, the error should be relatively small, and the analysis at least does not underestimate the crack width. In addition to the crack width analysis, the number of cracks, the maximum crack width and its location were manually checked on the photographic images (with the resolution of 30 μm per pixel) by using an image processing software ImageJ, and the results were verified by comparing them with computed ones.

3. Results and discussion

3.1. Compressive and tensile properties

Table 4 lists the experimental results of mechanical testing. Compressive and tensile strength are moderate, in the range of 17.4–27. 6 MPa and 2.9–3.4 MPa, respectively. Tensile strain capacities are very high in all groups. By utilizing temperature curing, tensile ductility could be improved up to 4.3%, which is several hundred times that of normal cement or geopolymer concrete. Temperature curing also enhances strength, and the T60-8 specimens exhibit the highest value, up to 27.6 MPa. Fig. 5 shows stress–strain curves obtained from dogbone testing. The strain hardening behavior can be clearly seen in all cases. Compared with ECC materials, developed geopolymer composites have slightly lower strength, but comparable or better tensile ductility. Therefore, the intended strain-hardening property of a geopolymer composite has been experimentally confirmed.

3.2. Crack pattern analysis by DIC

Fig. 6 shows the stress–strain curve of an additional specimen prepared for DIC analysis. The tensile strength is 3.6 MPa, and tensile strain capacity is 4.6%. Strain maps for different strain levels are obtained as shown in Fig. 7. Multiple cracks are clearly seen and saturated over the area of interest as the strain level increases. It should also be noted that cracks are not localized even under a high imposed strain condition. Therefore, the developed geopolymer composite possesses similar ductile characteristics as ECC materials.

Crack width analysis results are shown in Table 5. The number of cracks, average crack width and its standard deviation are those for cracks with larger than 20 μm width. Smaller cracks are found in the analysis, but not accounted for in the crack width calculation to avoid computational errors and errors due to the non-crack local high strains, as mentioned above. For verification, the number of cracks was counted manually in their digital images, and it is approximately the same as that computed. It is possible that the true number of cracks, average crack width and its standard deviation are slightly different from those computed. However, cracks with less than 10 μm width are so small that their effects on mechanical and durability performances would be insignificant.

According to the analysis results, the maximum crack width increases by about 50% (from 79 to 117 μm) between 1.0% and 4.5% strain levels, while the number of cracks increases by almost 300% (from 12 to 45). The average crack width is maintained at almost the same level of about 45 μm during straining from 1.0% to 4.5%. In terms of the average crack width, the developed geopolymer composites have better performance than various ECC materials. Therefore, it is highly likely that the geopolymer composites have improved durability, analogous to ECC materials, due to the tightly controlled crack width. Further investigations are required to verify the durability performance of the composite.

Table 5
Crack width distributions computed from DIC analysis.

Strain level (%)	Number of cracks[a]	Maximum crack width (μm)	Average crack width[a] (μm)
1.0	12	79	47 ± 17
2.0	27	83	43 ± 17
3.0	36	92	47 ± 19
4.0	43	100	45 ± 22
4.5	45	117	45 ± 23

[a] Only cracks whose widths are larger than 20 μm are counted, averaged and analyzed for the variance.

4. Conclusion

The hypothesis that brittle geopolymer could be made ductile with appropriate fiber reinforcement has been verified. The mechanical properties and multiple crack pattern during tensile loading were investigated in this study. The following findings were obtained:

- Strain hardening behavior with tensile ductility over 4% could be achieved.
- Temperature curing improves both strength and ductility properties. Compressive strength, tensile strength and tensile ductility could be increased up to 27.6 MPa, 3.4 MPa, and 4.3% on average, respectively.
- Multiple cracking pattern development can be easily visualized by strain maps obtained from DIC analysis.
- Cracks are distributed over the intended area of interest on the specimen surface with tightly controlled crack width even under a high imposed strain. The maximum and average crack widths are 117 μm and 45 μm, respectively, at 4.5% strain for a specimen with the strain capacity of 4.6%.

The developed geopolymer composites possess low to moderate strength and very high tensile ductility. Therefore, ductile geopolymer composite has been demonstrated to be feasible. Due to the tight crack width, improved durability performances are also expected. Regarding the compressive strength, further improvement could be possible by using different types of fly ash, higher curing temperature, longer curing duration, etc. Further studies are required to verify durability properties and achieving higher compressive strength.

Acknowledgements

Support from the National Science Foundation (Grant CMMI 1068005 to the University of Michigan) is gratefully acknowledged. The authors also acknowledge the material suppliers Headwaters, Lafarge, PQ Corporation, Kuraray and U.S. Silica for providing materials used in this study.

References

[1] Scrivener KL, Kirkpatrick RJ. Innovation in use and research on cementitious material. Cem Concr Res Feb. 2008;38(2):128–36.
[2] Duxson P, Provis JL, Lukey GC, van Deventer JSJ. The role of inorganic polymer technology in the development of 'green concrete'. Cem Concr Res 2007;37(12):1590–7.
[3] Tempest B, Sanusi O, Gergely J, Compressive strength and embodied energy optimization of fly ash based geopolymer concrete, In: Proceedings of 2009 World of Coal Ash conference, WOCA 2009, Lexington, KY. May 2009. p. 4–7.

[4] Provis JL, van Deventer JSJ. Geopolymers: structure, processing, properties and industrial applications. Cambridge (UK): Woodhead Publishing; 2009.
[5] Toledo Filho RD, Silva FA, Koenders EAB, Fairbairn EMR, editors. In: 2nd International RILEM conference on strain hardening cementitious composites (SHCC2-Rio). RILEM Publications SARL. 2011.
[6] Japan Concrete Institute, In: Proceedings of the JCI International Workshop on Ductile Fiber Reinforced Cementitious Composites (DFRCC). 2002.
[7] G.P.A.G. Van Zijl, F.H. Wittmann. Durability of strain-hardening fibre-reinforced cement-based composites (SHCC). RILEM State Art Rep 2011;4.
[8] Silva FJ, Thaumaturgo C. Fiber reinforcement and fracture response in geopolymeric mortars. Fatigue Fract Eng Mater Struct 2002;26:167–72.
[9] Zhao Q, Nair B, Rahimian T, Balaguru P. Novel geopolymer based composites with enhanced ductility. J Mater Sci 2007;42:3131–7.
[10] Sun P, Wu H-C. Transition from brittle to ductile behavior of fly ash using PVA fibers. Cem Concr Compos 2008;30:29–36.
[11] Yunsheng Z, Wei S, Zongjin L, Xiangming Eddie Z, Chungkong C. Impact properties of geopolymer based extrudates incorporated with fly ash and PVA short fiber. Constr Build Mater 2008;22:370–83.
[12] Lin T, Jia D, He P, Wang M. In situ crack growth observation and fracture behavior of short carbon fiber reinforced geopolymer matrix composites. Mater Sci Eng: A 2010;527:2404–7.
[13] Lin T, Jia D, He P, Wang M, Liang D. Effects of fiber length on mechanical properties and fracture behavior of short carbon fiber reinforced geopolymer matrix composites. Mater Sci Eng: A 2008;497:181–5.
[14] Lee BY, Cho C-G, Lim H-J, Song J-K, Yang K-H, Li VC. Strain hardening fiber reinforced alkali-activated mortar – a feasibility study. Constr Build Mater 2012;37:15–20.
[15] JSCE. Recommendations for design and construction of high performance fiber reinforced cement composites with multiple cracks. Tokyo: Japan Soc. of Civil Engineers; 2008.
[16] Ranade R, Stults MD, Li VC, et al. Development of high strength high ductility concrete. In: Proc second int'l RILEM conference on strain hardening cementitious composites (SHCC2), Rio de Janeiro, Brazil: 2011. p. 1–8.
[17] Sutton M, Orteu J, Schreier H. Image correlation for shape, motion and deformation measurements: basic concepts, theory and applications. Boston (MA): Springer US; 2009.
[18] Alam S, Loukili A. Application of digital image correlation to size effect tests of concrete. Int Conf Fract Mech Concr Concr Struct 2010.
[19] Kozicki J, Tejchman J. Experimental investigations of strain localization in concrete using Digital Image Correlation (DIC) technique. Arch Hydro-Eng Env Mech 2007;54(1):3–24.
[20] Shah SG, Chandra Kishen JM. Fracture properties of concrete–concrete interfaces using digital image correlation. Exp Mech May 2010;51(3):303–13.